

## Problem of ship shell durability

## Problem wytrzymałości powłoki statku

**Evgeny P. Burakovsky, Pavel E. Burakovsky**

Kaliningrad State Technical University, 236000, Kaliningrad, Sovietsky pr. 1, Russia  
e-mail: e\_burakovsky@mail.ru

**Key words:** spot of load, elasto-plastic deformation, experiment research, goffering, risk, bearing capacity

### Abstract

The article concerns the improvement of engineering calculation and refinement of durability margins of ship hull plane elements. Main results had been collected through vast experiments on tin construction-like models and half natural size structures. Results allow the refinement of areas' allocation of "flexible" and "rigid" links of plane elements under local span loading and function estimation of failure deflexion of plane of longitudinal rigidity, which is provided by the structure in the area of local deformation. Work results can be used to revise engineering calculations and refine the norms of defect survey. Wide usage of such survey norms can lead to ship repair time reduction and improve operational efficiency.

**Słowa kluczowe:** punkt nacisku, deformacje sprężysto-plastyczne, badania eksperymentalne, karbowanie, ryzyko, wytrzymałość

### Abstrakt

Artykuł dotyczy poprawy obliczeń inżynierskich i udoskonalenia marginesów trwałości elementów kadłuba statku. Rezultaty otrzymano po przeprowadzeniu wielu eksperymentów wykonanych na blaszanych modelach w skali 1:2. Zebrane wyniki pozwalają na udoskonalenie rozmieszczenia obszarów „elastycznych” i „sztywnych” połączeń elementów płaszczyzny będących pod miejscowym naciskiem i oszacowanie awaryjności wzdłużnej sztywności tej płaszczyzny, która jest wskazana przez strukturę w obszarze miejscowej deformacji. Rezultaty pracy mogą być wykorzystane do zmiany obliczeń inżynierskich i udoskonalenia norm badania wad. Szerokie wykorzystanie tych norm może prowadzić do skrócenia czasu naprawy statku i poprawy efektywności operacyjnej.

## Introduction

Ship operation is accompanied by in-service defects, which includes plastic deformation of structural elements. Most common defect in that class is shell goffering, which is induced by an intensive locally distributed loads. Ship structure goffering is by itself not dangerous, because value of goffering should not be greater then rated values [1], which are set according to degree of plastic deformation of structure.

But life cycle of the ship may produce extreme cases such as ice accretion. In such case, which shows marine experience [2], the most reasonable remedy is moving into ice, where ice accretion nearly stops. This remedy is now still widely used,

but ships in ice shelter usually do not have sufficient ice class which leads to board shell damage with deformation values more then rated. That can lead to a case of ship and crew loss when ship stability becomes insufficient, or hull breach and flooding of holds. Key problem of this article is investigation of deformed board shell plate strength, estimation of risks of its failure with given intensive locally distributed loads.

Besides, refinement of engineering calculation methods for ship structure including plates in elasto-plastic mode is linked with the refinement of area estimation working as rigid and flexible elements. Traditional method for plate structures used from the time of I.G. Bubnov for deformation compatibility equation of rigid and flexible elements for

equivalent girder in second approximation was successfully used for deformation analysis of locally loaded plate working in elasto-plastic mode. Based upon analysis of locally loaded structure deformation, calculated using numerical methods [3], E.A. Pavlinova proposed relations which allow calculating proportion of plate elements working as a flexible element, according to spot of load.

$$b_r = \frac{b_H}{\Psi_H} \tag{1}$$

$$\begin{cases} \Psi_H = \sin \left[ \frac{\pi}{4} \cdot \left( \frac{b_H}{a} + 0.25 \right) \right] & \text{for } \frac{b_H}{a} \leq 1.75 \\ \Psi_H = 1 & \text{for } \frac{b_H}{a} > 1.75 \end{cases} \tag{2}$$

where:  $b_r$  – width of flexible area,  $b_H$  – width of load spot,  $a$  – transversal spacing,  $\Psi_H$  – reduction load coefficient of middle strip beam, considering supporting influence of unloaded parts and transversal bearing edges.

However, use of numerical calculations for big elasto-plastic deformations of locally loaded planes requires experimental conformation. It was decided to hold an experiment. For that reason series of construction-like tin models and special bed were constructed. Model loading was carried out by different male cores via elastic washer (Fig. 1).

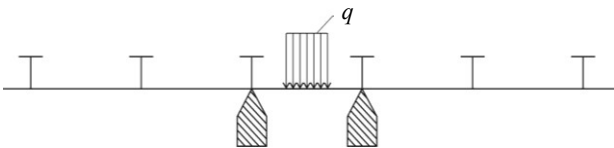


Fig. 1. Loading model diagram  
Rys. 1. Schemat modelu załadowania

Strain distribution registration was made using strain gauging. Strain gauges were put on two sides of a plane in direction of shorter side to be able to detect bending and chain forces. To ensure gauges operational reliability they were put along the line of plane bending (Fig. 2).

Loading was made by steps, on each of it bending deflection and strain distribution were registered. Typical diagram of chain force distribution is shown on figure 3. Draws attention the fact that change of sign of chain force appears nearly on the same area, irrespective of plane load value, which means that proportion of rigid and flexible elements does not vary in the process of deformation.

Experiments allowed to formulate a relation for flexible beam width in accordance with spot of load:

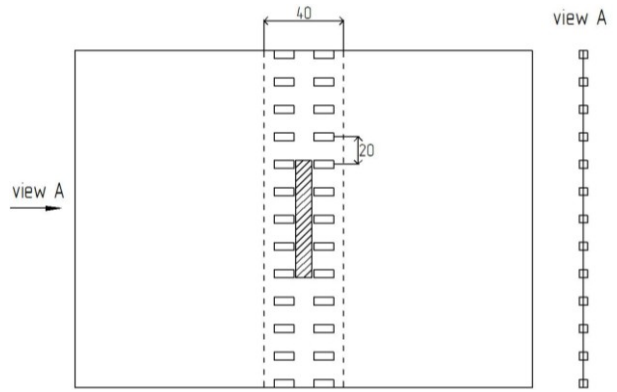


Fig. 2. Loading model and strain gauges arrangement  
Rys. 2. Model załadowania i układ wskaźników

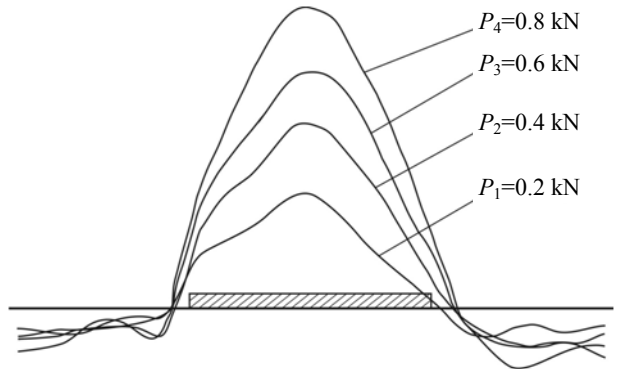


Fig. 3. Chain force diagram  
Rys. 3. Wykres siły łańcuchowej

$$b_r = \sqrt{b_H} \cdot \left( 2 \cdot e^{\frac{b_H^{1.5}}{15}} + \sqrt{b_H} \right) \tag{3}$$

where designations correspond with that in formulae (1) and (2).

Graphical version of this relation is shown on figure 4 as curve 2 along with flexible beam width variation according to load spot by relation of E.A. Pavlinova (1). Curves show that for given load areas  $\bar{b}_H = 0.5 \div 2$  inaccuracy of flexible beam

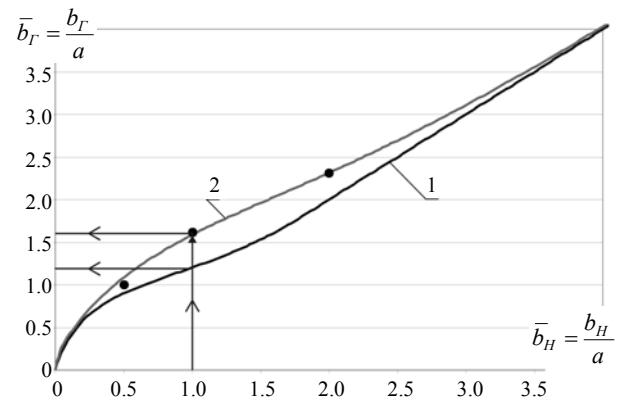


Fig. 4. Flexible area width in relation to load spot size diagram  
Rys. 4. Szerokość obszaru elastycznego w stosunku do schematu wielkości miejsca załadowania

width can be quite big. As for  $\bar{b}_H = 1$  formulae (1) and (2) give the value  $\bar{b}_r = 1.2$  but formula (3) gives  $\bar{b}_r = 1.6$ . As it can see, inaccuracy may be up to 33% which is unacceptable as it lowers calculation accuracy a lot.

It was decided to verify model experiment results on half-scale structures. For that purpose series of half normal size constructions were made with 5 mm wall thickness. Experiments were made on 500 ton press machine PMM-500. Experimental installation is shown on figure 5.

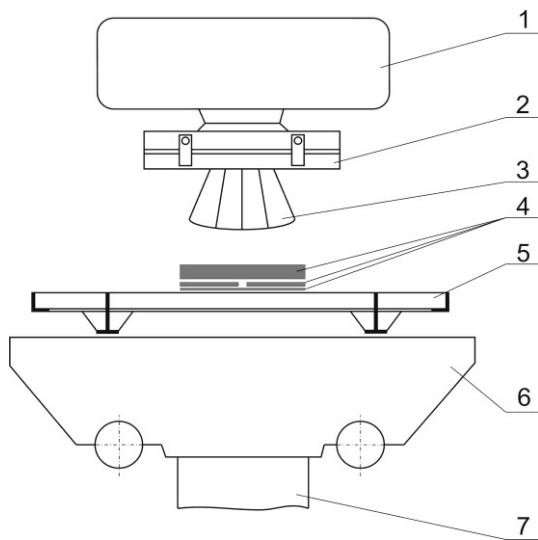


Fig. 5. Half-sized span loading scheme: 1 – upper cross-beam, 2 – male core mounting system, 3 – male core, 4 – washers, 5 – span under test, 6 – trolley, 7 – lower movable cross-beam

Rys. 5. Schemat częściowej rozpiętości załadunku: 1 – górna belka, 2 – rdzeń systemu mocowania, 3 – rdzeń, 4 – podkładka, 5 – testowana rozpiętość, 6 – wózek, 7 – niższa ruchoma belka

Diagram of the span under test with dimensions 800×2000 mm is shown on figure 6. Span includes two *T* beam stiffeners with 6×80/6×60 and *T* beam pieces of the web framing with 6×120/6×60. Distance between stiffeners is 400 mm, between web elements – 1200 mm. Material used – steel 4c. Mechanical characteristics of steel were obtained from tensile test. Boundary conditions are fulfilled by welding an *L*-bar to the perimeter of the span.

During the test locally distributed on the area of 200×400 mm transversal load was applied to span. Application area was located between neighbour stiffeners, longer side of area in parallel with them. Uniform load was realized by guiding force from press machine to span via rigid male core with curvature radius of 500 mm and 50 mm thick rubber washers beneath it to uniform the load.

Deformation registration was made using strain gauges with 10 mm base. Registration was performed using digital strain gauge meter CTM. Sensors for chain force distribution were glued on two sides of plane along the line of bending similar to diagram on figure 2. Bending deflection was measured by mercer clock gauge with division value 0.01 mm. Loading was performed in steps of 30, 60, 90, 120, 150 kN. On each step overloading of 1.0–1.5% was produced for 1 to 2 minutes then span was unloaded to given value and bending deflections and force distribution was measured as is shown on figure 7.

Experiment results for half-sized structures given in this article and [4] conform well to that of model experiments, which allows recommending relation (3) for practical use.

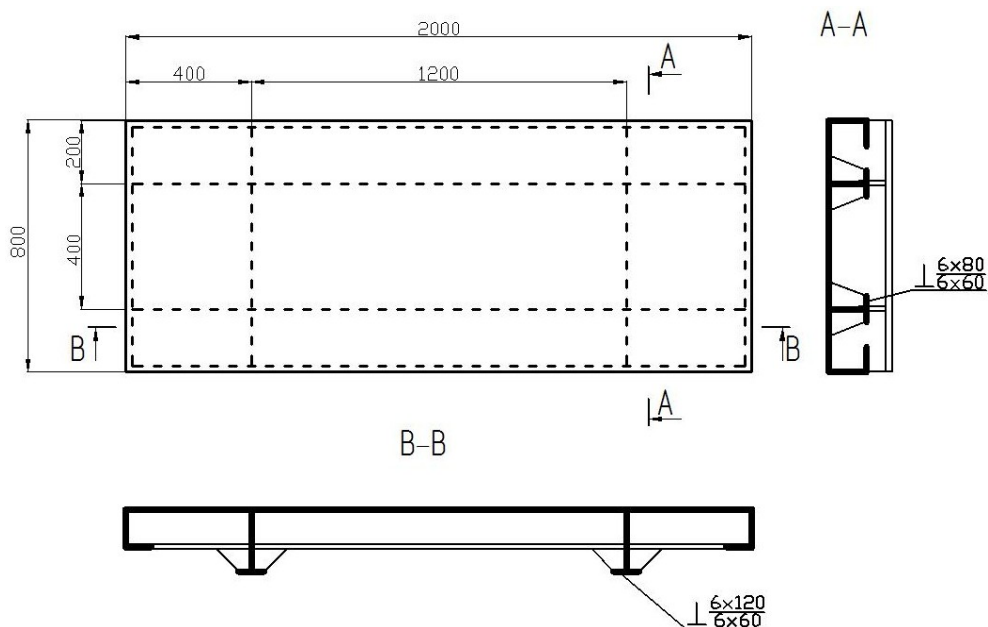


Fig. 6. Span under test diagram

Rys. 6. Schemat rozpiętości testowej

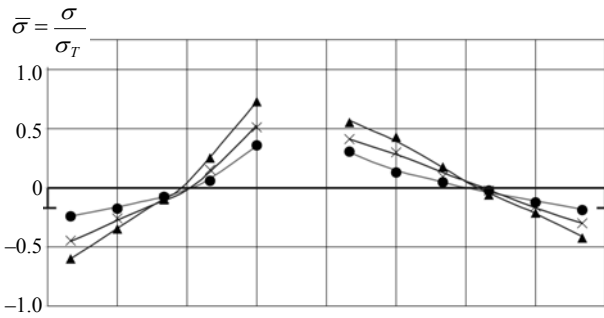


Fig. 7. Chain force distribution in half-sized span  
Rys. 7. Rozkład siły łańcuchowej w rozpiętości połowicznej

Commonly process of collapsing is influenced by variety of factors connected with material mechanical characteristics. One of the significant factors defining the geometry of plane failure is the thrust coefficient. Thrust rigidity estimation of planes working in locally loaded span (Fig. 8 –  $b$  – height,  $l_1$  – length) according to [4] shows that thrust rigidity value, shown by thrust coefficient, depends greatly on spot orientation:

$$K_P = \frac{0.08 + 0.6 \frac{l_1}{b}}{1.08 + 0.6 \frac{l_1}{b}} \quad (4)$$

where:  $b$  – height of punch,  $l_1$  – length of punch.

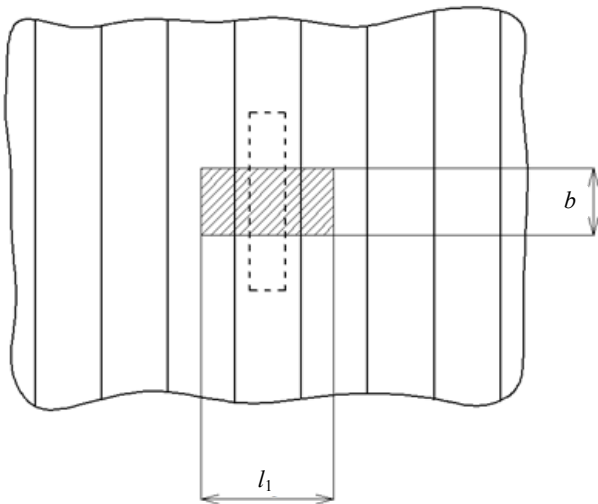


Fig. 8. Board span loading diagram  
Rys. 8. Schemat rozpiętości załadowania na pokładzie

According to Register Rules [5] loads are applied to a spot transverse to ribs. This gives quite high thrust coefficient values according to (4) but in the presence of goffering value dramatically drops (Table 1, where:  $W_0$  – residual bending deflection of neighbour spacings referred to plane thickness). Tendency is visible that higher goffering values lead to lower plane thrust values (Fig. 9). Bending deflections influence on thrust rigidity was ac-

Table 1. Locally loaded plane thrust coefficient variation with variation of load spot geometry and bending deflections of neighbour spacings – numerical data

Tabela 1. Zmienność współczynnika lokalnego załadowania powierzchni nacisku ze zmiennością geometrii miejsca obciążenia i odchylenia wygięcia sąsiednich rozstawów – dane liczbowe

$\frac{l_1}{b}$	$K_P(\bar{W}_0)$					
	$\bar{W}_0 = 0$	$\bar{W}_0 = 1$	$\bar{W}_0 = 2$	$\bar{W}_0 = 3$	$\bar{W}_0 = 4$	$\bar{W}_0 = 5$
2.5	0.61	0.507	0.443	0.398	0.362	0.321
2.0	0.56	0.455	0.39	0.348	0.316	0.291
1.5	0.495	0.39	0.33	0.29	0.26	0.239
1.0	0.405	0.306	0.253	0.22	0.2	0.18
0.5	0.275	0.2	0.16	0.134	0.12	0.106

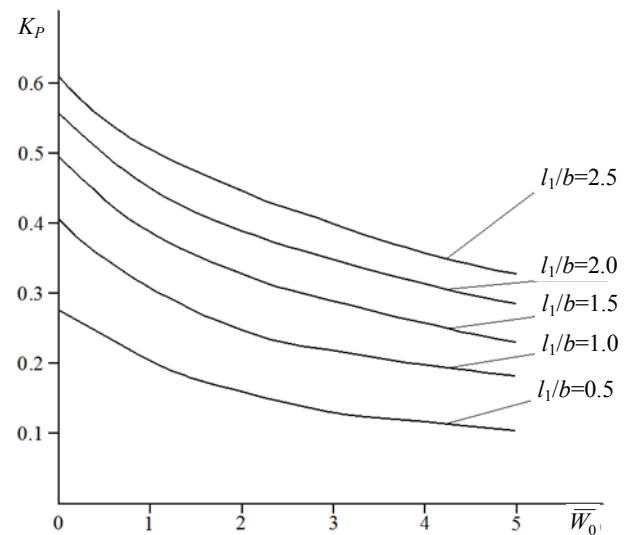


Fig. 9. Graph of locally loaded plane thrust coefficient variation with variation of load spot geometry and bending deflections of neighbour spacings

Rys. 9. Wykres zmienności współczynnika lokalnego załadowania powierzchni nacisku ze zmiennością geometrii miejsca obciążenia i odchylenia wygięcia sąsiednich rozstawów

counted in accordance with [4] using correction coefficient:

$$K_{W_0} = 1 + 0.7 \frac{\bar{\sigma}_0 + 2}{(1 + \bar{\sigma}_0)^2} \left( \frac{W_0}{\delta} \right)^2 \quad (5)$$

where:  $\bar{\sigma}_0$  – chain force on the punch border in strip beam referred to its Euler tensions,  $W_0$  – residual bending deflection of neighbour spacings,  $\delta$  – plane thickness.

Therefore, area of deformation and failure under study is located with thrust rigidity values lower than  $K_P = 0.3$ .

Experiments were held on construction-like tin models. Part of a board span was modeled consisting of shell and frame beams. Spans were loaded by male core in the spacing with longer side orientated along the framework (see dash line on figure 8). Size of male core was chosen to give plane thrust

rigidity range  $K_p < 0.3$ . Loading was performed in steps after each unloading was performed with residual bending deflection measurement using mercer dial gauge. In the experiment planes could not be collapsed without frame deformation, so loading was performed from the frame side of the span. In the plane of framework fixed supports were placed. Scheme is shown on figure 1.

Plane collapse experiment series in the practical range of thrust rigidity  $K_p = 0.13 \div 0.28$  allowed to refine plane collapse behaviour. It was cleared that with lowering thrust properties of the plane bending deflection at the moment of collapse increases slightly. Thus, with the thrust coefficient  $K_p = 0.28$  bending deflection is  $W_p/a = 0.21$  and with  $K_p = 0.13$  bending deflection is  $W_p/a = 0.26$ , where  $W_p$  is bending deflection at the moment of collapse,  $a$  – transversal spacing.

Such behaviour is similar for planes irrespective to their thickness. Result allows stating that dangerous bending deflections for planes with goffering is higher then for plane without goffering and higher thrust rigidity. Collapse bending deflections of a span (expectation) in thrust rigidity range  $K_p = 0.1 \div 1$  may be approximated by:

$$\left\{ \begin{array}{l} \frac{W_p}{a} = \\ = (1.8K_p^2 - 0.81K_p + 0.41) \sin^{1.8} \left[ \frac{\pi}{4} (2.5 + 1.25K_p) \right] \\ \quad \text{for } K_p \leq 0.55 \\ \frac{W_p}{a} = 0.2 \quad \text{for } K_p > 0.55 \end{array} \right. \quad (6)$$

According to formulae (4) and (5) thrust rigidity value can be calculated for goffered spans. Using

(6) collapse probability can be estimated taking normal distribution as a distribution of collapse bending deflections of a span. Bending deflection measurement ( $W_\phi$ ) and integration of area beneath probability density curve to given bending deflection  $W_1$  (figure 10) allows to estimate collapse risk of a span taking into account predicting actual bending deflection reaches given deflection  $W_1$  according to:

$$Q_p = \int_0^{W_1} \varphi(W_p) dW_p \quad (7)$$

where:  $Q_p$  – span collapse probability,  $W_1$  – bending deflection according to [4],  $\varphi(W_p)$  – probability density of collapse bending deflection, measured experimentally.

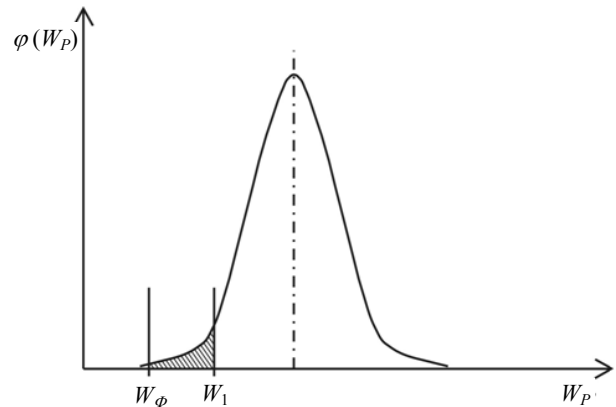


Fig. 10. Span collapse risk estimation  
Rys. 10. Oszacowanie ryzyka rozpadu rozpiętości

Shown approaches can be successfully used in refining the norms of goffering with probability criteria. Graphic view of norming method is shown on figure 11. Here, line 1 represents admissible bending deflections of a span [1], line 2 – expecta-

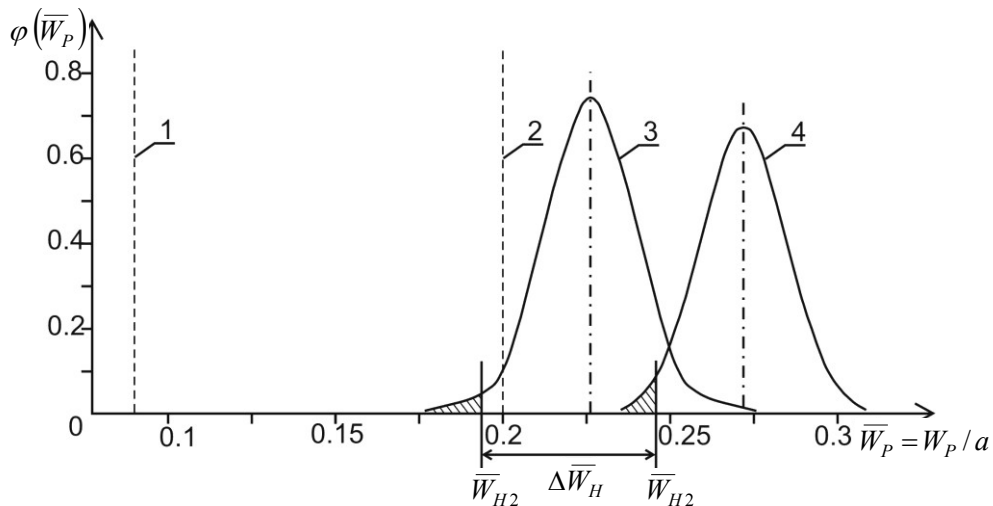


Fig. 11. Goffering regulation method  
Rys. 11. Metoda regulacji gofferingowej

tion of collapse bending deflections, made by L.M. Belenkiy for absolutely rigid thrust [6], line 3 – probability density for collapse deflections with  $K_p = 0.28$ , line 4 – probability density for collapse deflections with  $K_p = 0.13$ . Taking left parts of density curve, corresponding to standard probability of span collapse, and integrating them corresponding bending deflections can be received. Comparison of these values shows that for given probability of collapse line 4 (for structure with developed goffering) gives up to 30% higher standard bending deflection than line 3.

Shown bending deflection regulations method corresponds to locally distributed operational load, when area of load is smaller than spacing. Actual load areas (especially ice loads) may be longer, spreading lengthwise for 2–4 spacings, which increases thrusting characteristics of a span. In this case  $\Delta \bar{W}_H$  will be little lower, about 10–15% of  $\bar{W}_H$ . Using probabilistic methods for regulation

of operational defects allows more precise estimation of bearing capacity of ship structure.

Given research shows additional bearing capacity reserve for damaged structure. Use of given regulation method allows to decrease repair work needed which in turn increases operational efficiency of a ship.

## References

1. Pravila klassifikacionnyh osvidetel'stvovaniy sydov v èkspluatácii. Roccijckij Morskoy Registr Sudohodstva. SPb., 2010.
2. Buânov N.F.: Plavanie sydov v tâželyh usloviâh. Dal'nevostočnoe knižnoe izdatel'stvo, Vladivostok 1968.
3. Kurdûmov V.A., Trâskin V.N.: Uprugoplastičeskij izgib obšivki ledovogo poâsa. Trudy LKI. Ledoprohodimost' i ledovaâ pročnost' morskikh sudov. L., 1979.
4. Burakovsky E.P.: Soveršenstvovanie normirovaniâ parametrov èkspluatacionnyh defektov korpusov sudov. KGTU, Kaliningrad 2005.
5. Pravila klassifikacii i postrojki morskikh sudov. Rossijskij Morskoy Registr sudohodstva. T. 1. SPb., 2005.
6. Belen'kij L.M.: Bol'shie deformacii sudovyh konstrukcij. L.: Sudostroenie, 1973.